Astronomy & Astrophysics manuscript no. AMIGAIX-21Apr2011-final
July 5, 2011

© ESO 2011

arXiv:1107.0601v1 [astro-ph.CO] 4 Jul 2011

The AMIGA sample of isolated galaxies

VIII. The rate of asymmetric H I profiles in spiral galaxies †⋆

D. Espada[1,2], L. Verdes-Montenegro[1], W. K. Huchtmeier[3], J. Sulentic,[1], S. Verley[4], S. Leon[5], and J. Sabater[1,6]

[1] Instituto de Astrofísica de Andalucía (IAA-CSIC), Apdo. 3004, 18080 Granada, Spain
[2] National Astronomical Observatory of Japan (NAOJ), 2-21-1 Osawa, Mitaka, Tokyo 181-8588, Japan; e-mail: `daniel.espada@nao.ac.jp`
[3] Max-Planck-Institut fuer Radioastronomie, Postfach 2024, D-53010 Bonn, Germany
[4] Dept. de Física Teórica y del Cosmos, Universidad de Granada, Spain
[5] Joint ALMA Observatory/ESO, Av. Alonso de Córdova 3107, Vitacura, Santiago, Chile
[6] Institute for Astronomy, University of Edinburgh, Edinburgh EH9 3HJ, UK

Received; accepted

ABSTRACT

Context. Measures of the H I properties of a galaxy are among the most sensitive interaction diagnostic at our disposal. We report here on a study of H I profile asymmetries (e.g., lopsidedness) in a sample of some of the most isolated galaxies in the local Universe. This presents us with an excellent opportunity to quantify the range of intrinsic H I asymmetries in galaxies (i.e., those not induced by the environment) and provides us with a zero-point calibration for evaluating these measurements in less isolated samples.
Aims. We aim to characterize the H I profile asymmetries in a sample of isolated galaxies and search for correlations between H I asymmetry and their environments, as well as their optical and far infrared (FIR) properties.
Methods. We use high signal-to-noise global H I profiles for galaxies in the AMIGA project (Analysis of the Interstellar Medium of Isolated GAlaxies, `http://amiga.iaa.es`). We restrict our study to $N = 166$ galaxies (out of 312) with accurate measures of the H I shape properties. We quantify asymmetries using a flux ratio parameter.
Results. The asymmetry parameter distribution of our isolated sample is well described by a Gaussian model. The width of the distribution is $\sigma = 0.13$, and could be even smaller ($\sigma = 0.11$) if instrumental errors are reduced. Only 2% of our carefully vetted isolated galaxies sample show an asymmetry in excess of 3σ. By using this sample we minimize environmental effects as confirmed by the lack of correlation between H I asymmetry and tidal force (one-on-one interactions) and neighbor galaxy number density. On the other hand, field galaxy samples show wider distributions and deviate from a Gaussian curve. As a result we find higher asymmetry rates ($\sim$ 10–20%) in such samples. We find evidence that the spiral arm strength is inversely correlated with the HI asymmetry. We also find an excess of FIR luminous galaxies with larger HI asymmetries that may be spirals associated with hidden accretion events.
Conclusions. Our sample presents the smallest fraction of asymmetric H I profiles compared with any other yet studied. The width of the associated asymmetry parameter distribution can help to distinguish the frequency and processes of self-induced HI asymmetries, and serve as a baseline for studying asymmetry rates in other environments.

Key words. galaxies: evolution – galaxies: interactions – galaxies: ISM – surveys – H I : galaxies

1. Introduction

The geometry and kinematics of gaseous disks in galaxies are mainly governed by the gravitational potential of stellar and non-baryonic components. Any perturbation of the equilibrium caused by either internal or external processes, may produce asymmetries in these disks. Atomic gas (H I) is the most extended cold component of the interstellar medium (ISM) and is a sensitive diagnostic of perturbations. The H I component in spiral galaxies has long been known to show both geometrical and kinematic asymmetries (e.g., Beale & Davies 1969; Huchtmeier 1972; Allen et al. 1973; Baldwin et al. 1980). Asymmetries in stellar disks are also common and are traced by optical and near-infrared light (the latter less affected by dust extinction). Observations show that 30% of galaxies are significantly *lopsided* at near-infrared wavelengths (Block et al. 1994; Rix & Zaritsky 1995; Zaritsky & Rix 1997; Bournaud et al. 2005). Asymmetries in the stellar component are not necessarily correlated with lopsidedness in the gaseous component (Kornreich et al. 2000; Wilcots & Prescott 2004). This lack of correlation is not surprising because the neutral hydrogen component in a galaxy is typically twice as extended as the stellar component (e.g., Broeils & van Woerden 1994), and might be perturbed in different ways with respect to the stellar component (e.g., stripping). The study of H I properties is thus a better probe of past and/or recent perturbations than the stellar counterpart, especially for weak interactions.

Send offprint requests to: D. Espada

⋆ Based on observations with the 100-m telescope of the MPIfR (Max-Planck-Institut fuer Radioastronomie) at Effelsberg, GBT under NRAO (the National Radio Astronomy Observatory is a facility of the National Science Foundation operated under cooperative agreement by Associated Universities, Inc.), Arecibo Observatory (National Astronomy and Ionosphere Center, which is operated by Cornell University under a cooperative agreement with the National Science Foundation) and the Nançay Observatory. † Full Table 1 is available in electronic form at the CDS via anonymous ftp to `cdsarc.u-strasbg.fr (130.79.128.5)` or via `http://cdsweb.u-strasbg.fr/cgi-bin/qcat?J/A+A/vvv/ppp` and from `http://amiga.iaa.es`.

Study of global H I velocity profiles of galaxies has proven to be very useful for a quantification of the frequency and amplitude of disk asymmetries (e.g. Richter & Sancisi 1994). While only aperture synthesis can provide full 2D information about the H I distribution and kinematics, the 1D profiles provide a valuable measurement at a small fraction of the cost in observing time.

Past work suggests that the H I asymmetry properties of galaxies do not depend strongly on local environmental conditions. Studies of *field* and/or isolated galaxies suggest that *at least 50 %* show significant H I profile asymmetries (Richter & Sancisi 1994; Haynes et al. 1998), and even higher ~75% in late-type spiral galaxies (Matthews et al. 1998). Although homogeneous studies of the asymmetry rate in richer environments are rare, it is usually believed that they show a comparable rate of asymmetric H I profiles.

The implications of a high asymmetry rate essentially independent of environment is currently the subject of debate (for a review see Jog & Combes 2009; Sancisi et al. 2008). It has been suggested that the mechanism responsible for producing asymmetric disks must be long-lived because high asymmetry rates are observed in samples of field and/or isolated galaxies. Because the signatures of tidal encounters are relatively short-lived, lasting only on the order of a dynamical time-scale for a wide range in mass ratios, orientations, inclinations, relative velocities and impact parameters (e.g. Bournaud et al. 2005), it cannot be the only agent responsible for the high asymmetry rate in different environments. A number of longer-lived mechanisms have been proposed, a) intermittent minor mergers (Walker et al. 1996; Zaritsky & Rix 1997), b) high-velocity cloud/gas accretion (Bournaud et al. 2005; Sancisi et al. 2008; Miller et al. 2008), c) halo-disk misalignment (Levine & Sparke 1998; Noordermeer et al. 2001) and/or d) internal perturbations including sustained long-lived lopsidedness owing to non-circular motions (Baldwin et al. 1980) or global m=1 instabilities (Saha et al. 2007).

In order to address the relevance of the different proposed mechanisms (internal versus external, short versus long-lived) one must first study a sample of well isolated galaxies in the nearby Universe ($\lesssim$ 150 Mpc). This approach should minimize any contribution from tidal interactions and facilitate the interpretation of results with respect to other samples of galaxies. Reference samples used to study the rate of H I asymmetries involve galaxies which, although assumed to be field/isolated, usually include a significant population of interacting galaxies (e.g. Richter & Sancisi 1994). Note that field galaxies are defined as galaxies not belonging to the cluster environment and a significant number of them are likely to be members of interacting pairs or multiplets (Sulentic et al. 2006). Richter & Sancisi (1994) find that about half of the nearby field galaxies show asymmetric profiles, estimated from a compilation of six H I surveys (1371 profiles were classified). It is important to remember that, 1) the overall environmental properties of the samples were not assessed meaning that a significant fraction of galaxies might be environmentally influenced, and 2) asymmetries were assessed using qualitative criteria (Richter & Sancisi 1994).

Statistical studies of H I asymmetries in large samples of galaxies selected according to a well defined isolation criterion and using an objective quantification are rare. The only existing systematic study of H I asymmetries in an isolated sample is that of Haynes et al. (1998), who studied the asymmetry rate for N = 104 (N = 78) galaxies that obey a 0.5^{o} (1^{o}) projected separation criterion with respect to any known companion in the Arecibo General Catalog (AGC, private database of R. Giovanelli and M. P. Haynes), where 0.5^{o} corresponds to 175 kpc at a typical velocity of the core sample at V$_r$= 1500 km s^{-1}. About half of the galaxies appear to show significant H I asymmetries. However, only companions with a velocity difference ΔV< 400 km s^{-1} relative to the primary are considered. The AGC is complete up to $m \sim 15.4$ mag and/or a diameter of 1′ (equivalent to a typical linear size of 6 kpc). The velocity criterion could make this sample biased against unbound plunging encounters, and owing to the size limit of the catalog, small galaxies would not have been taken into account – hierarchical systems of small galaxies may in principle produce significant asymmetries.

Other studied samples are composed of field galaxies. Matthews et al. (1998) studied a sample of N = 30 moderate to low surface brightness late-type spirals. Their galaxies lie between 2^{o} and 6^{o} from the center of the Fornax cluster or are field galaxies. They suggest that 77% of the H I profiles in their sample show a relevant asymmetry. Bournaud et al. (2005) studied N = 76 galaxies based on the OSUBS Galaxy Survey (Eskridge et al. 2002), a sample not selected according to any environmental criterion, which hence may have a relevant amount of interacting galaxies. However, it has been recently referred to as a field galaxy sample (e.g., Jog & Combes 2009). The asymmetry is larger than 10% for nearly 66% of the galaxies in this sample.

In this paper we use a large and complete sample of isolated galaxies (Verdes-Montenegro et al. 2005; Lisenfeld et al. 2007) to evaluate the intrinsic distribution of H I asymmetries. Comparisons show that our sample is more isolated than those used in previous studies and indeed is representative of the most isolated galaxies in the local Universe. The AMIGA project (Analysis of the interstellar Medium of Isolated GAlaxies[1], Verdes-Montenegro et al. 2005) involves vetting and analyzing the properties of galaxies in the Catalogue of Isolated Galaxies (N = 1050 galaxies, CIG, Karachentseva 1973), and provides a good starting point for this aim. This project includes a refinement of the sample through 1) revision of optical positions (Leon & Verdes-Montenegro 2003), 2) analysis of optical properties and completeness (Verdes-Montenegro et al. 2005), 3) revised optical morphologies (Sulentic et al. 2006) and 4) reevaluation of the isolation degree (Verley et al. 2007c,b). We use all these refinements in the present paper. The isolation criterion used for this compilation minimizes the probability of a major interaction within the last $\sim$ 3 Gyr (Verdes-Montenegro et al. 2005) while quantifying possible minor interactions. A multiwavelength characterization of different interstellar medium (ISM) components/phases and of the stellar component has been carried out including a) optical (Verdes-Montenegro et al. 2005), b) FIR (Lisenfeld et al. 2007), c) radio-continuum (Leon et al. 2008), and d) Hα emission (Verley et al. 2007a), as well as e) nuclear activity (Sabater et al. 2008, 2011).

This paper presents an analysis of global (1D) asymmetry measures for N = 312 H I AMIGA galaxies with high signal-to-noise (S/N) spectra (Sect. 2). We cleaned the sample of sources with uncertain asymmetry measures, yielding a total of N = 166 galaxies with high reliability data. For this subsample we studied the H I profile asymmetry rate (Sect. 3), the role of the environment for the rate of lopsided profiles (Sect. 4), as well as the correlations between H I asymmetry and stellar properties (optical luminosity, morphological type and signs of perturbation), and star formation rate (as traced by FIR luminostity, Sect. 5). Finally we identify the underlying distribution of intrinsic profile asymmetries and discuss the possible origin of asymmetries in gaseous disks (Sect. 6).

---

[1] `http://amiga.iaa.es`

2. The sample

2.1. Sample selection

This paper presents descriptions of the shape of H I profiles with special emphasis on the degree of asymmetry. We identified the galaxies with the highest S/N H I profiles in the AMIGA project, obtained from observations at the Arecibo, Effelsberg, Nançay and GBT radio-telescopes, as well as from a compilation from archives/literature. The H I spectra are available at `http://amiga.iaa.es`. We initially consider for this study those H I spectra with a signal-to-noise $S/N > 10$ (S/N obtained as the peak flux to rms ratio), in total $N = 383$ galaxies. A $S/N > 10$ is appropriate to gain a good estimate of the asymmetry (Tifft & Huchtmeier 1990).

In addition we further restricted the sample to galaxies with profiles with high-velocity resolution to total width ratio, $W_{20}/\Delta V > 10$, where W_{20} is the width at a 20% level and ΔV is the resolution of the H I profile. This criterion is necessary to ensure that the profiles are well sampled. As a side-effect, it partially excludes face-on and low mass/luminosity galaxies. We excluded sources with evidence of problems related to bad baseline subtraction and/or interference contamination. Finally we chose galaxies with recession velocities $V > 1500$ km s^{-1} to permit proper evaluation of the isolation. A prohibitively large region on the sky would be required to assess isolation for galaxies with $V < 1500$ (Verley et al. 2007c,b). In any case, they are all members of the Local Virgo Supercluster. Application of these restrictions yielded a sample of $N = 312$ isolated galaxies with high quality H I profiles. We will refer to this sample as the H I *sample*. We characterize profile asymmetry in two ways: 1) quality-based on visual inspection of the profiles and 2) quantity-based on an areal asymmetry index $A_{flux\ ratio}$ (Sect. 3). For a statistical analysis we performed a further refinement of the sample by considering only those galaxies with lowest uncertainty in their asymmetry parameter. This resulted in a final sample of $N = 166$ isolated galaxies, which we call the H I *refined subsample* (Sect. 3.4).

2.2. Basic properties of the samples

Figure 1 summarizes the basic optical/FIR properties of both the H I sample and the H I refined subsample. The different panels include recession velocity, morphological type as well as optical and FIR luminosity distributions. We compare these distributions with those corresponding to the optically complete sample, which was estimated to be 85–90 % complete to m_B= 15.0 mag, and is composed of $N = 719$ CIG galaxies (Verdes-Montenegro et al. 2005). The latter sample is appropriate to represent the entire population of isolated galaxies in the local Universe.

We summarize the dispersions of the basic properties for galaxies included in the different samples as well as the deviations between the H I samples and the optically complete sample:

- *a*) Radial velocity V (Verdes-Montenegro et al. 2005): Velocities range over 1dex in the three samples, covering the range 1500 km s^{-1} $< V <$ 14000 km s^{-1}. The H I refined subsample, and to a lower extent the H I sample, is slightly skewed toward lower velocities relative to the optically complete sample. The sample becomes seriously incomplete beyond 9000 km s^{-1}.
- *b*) Morphology $T(RC3)$ (Sulentic et al. 2006): Types are given in the RC3 numerical scale (de Vaucouleurs et al. 1991). The bulk of the CIG sample involves late-type galaxies in the range $3 < T < 7$ (Sb to Sd) with 2/3 of the sample in a very narrow range T=4±1 (Sb–Sc). Only 14% of the sample involve early-type systems, which suggests that our sample represents the extreme (low) end of the morphology-density relation. The H I refined subsample contains a higher percentage of late-type galaxies (especially Sb–Sc) than the optically complete sample. This is not surprising because earlier type galaxies have a systematically lower H I content than later types and are especially excluded by selecting those H I profiles with S/N > 10.
- *c*) Optical luminosity L_B (Verdes-Montenegro et al. 2005): With few exceptions the sample spans a 1 dex luminosity range ($9.5 < \log(L_B[L_\odot]) < 10.5$). Galaxies with $\log(L_B[L_\odot]) < 10$ are overrepresented in the H I sample (and H I refined subsample) likely because higher luminosity galaxies prefer the high-velocity tail of the sample (Malmquist effect) and often fall below m=15.0.
- *d*) FIR luminosity L_{FIR} (Lisenfeld et al. 2007): The three distributions are relatively similar to each other. The shape of the FIR luminosity distribution is flatter than the optical and shows a peak near log L_{FIR}= 9.6. The full range covers 2 dex ($8.5 < \log(L_{FIR}[L_\odot]) < 10.5$). The difference between the optical and FIR luminosity distributions likely reflects the extreme FIR ”quietness” of our very isolated galaxy sample. Only detections are shown in Figure 1.

3. H I profile shape and quantification of H I lopsidedness

In this section we present a general view of the H I profile shape and two ways of quantifying profile lopsidedness. First, we examine the profiles via visual inspection (see Sect. 3.1) using criteria similar to those employed in the largest H I profile shape study to date, Richter & Sancisi (1994). We then quantify the asymmetry level in a more objective manner using a numerical parameter (Sect. 3.2) and compare visual and numerical descriptions in Sect. 3.3.

3.1. H I profile shape and visual estimation of lopsidedness

Visual inspection of our H I sample shows that 88% show double horns with the rest showing single peaks that in most cases involve face-on spiral galaxies. We visually classified the profiles in the H I sample ($N = 312$ galaxies) as *symmetric*, *slightly asymmetric*, and *strongly asymmetric*, in a similar way as Richter & Sancisi (1994), who studied a sample of $N = 1371$ spectra (equivalent, respectively, to their notation as *No*, *Weak* and *Strong*). We find that $N = 141$ galaxies show symmetric H I profiles (45 %), $N = 126$ sligthly asymmetric profiles (40%), and $N = 45$ strongly asymmetric profiles (15%). In order to illustrate this visual classification we show some examples of symmetric, slightly asymmetric, and strongly asymmetric H I profiles in Figures 2, 3, and 4, respectively. Based on the visual classification, our sample appears to show similar average rates as those obtained by Richter & Sancisi (1994): 47 ± 5 %, 34 ± 6 %, and 19 ± 6 %.

The most common asymmetry found in our sample involves unequal peaks in the double horn profiles. The most extreme H I asymmetries occur for 43 galaxies (out of 312) where the peak flux difference is approximately larger than 25%. Only one of them has a peak flux difference larger than 50% (CIG 317). Some galaxies with double peaked profiles show peculiarities: CIG 144 shows a central peak stronger than the horns of the double peaked profile, CIG 858 shows a profile with a peculiar central trough, CIGs 238, 382, 928, and 1029 show apparent wings (significant excess flux –3σ– within a 50 – 100 km s^{-1} wide) beyond the outer walls of the double-horn profile. CIG 170 shows an uncommon flat H I profile. CIG 870 may also have wings that are 50 – 100 km s^{-1} wide, although it seems to be a face-on galaxy. The observed wings may indicate a projected gas-rich companion or extra-planar motions owing to a nurture event.

3.2. Integrated density flux ratio parameter ($A_{flux\ ratio}$)

A variety of parameters have been used in the literature to quantify the asymmetry level in H I profiles. We employ an areal asymmetry index to quantify profile lopsidedness, namely the integrated flux density ratio $A_{flux\ ratio}$ (e.g. Haynes et al. 1998, Kornreich et al. 2001), defined as $A_{flux\ ratio} = A_{l/h}$, if $A_{l/h} > 1$, and $1/A_{l/h}$ otherwise, where $A_{l/h}$ is the ratio of the areas under the profile at velocities lower (S$_l$) and higher (S$_h$) than the central velocity (V_m):

$$A_{l/h} = \frac{S_l}{S_h} = \frac{\int_{V_l}^{V_m} S_v dv}{\int_{V_m}^{V_h} S_v dv},$$

where V_l and V_h represent the low and high velocities measured at 20% intensity level with respect to the peak. V_m is calculated as the mean velocity at the same level, $V_m \mathbf{= (}V_h\mathbf{+}V_l\mathbf{)/2}$. Note that $A_{flux\ ratio}$ is invariant to the sense of rotation of the galaxy. We use this parameter since it is the most common asymmetry index that can be found in the literature and allows us to compare our results with other samples of galaxies (see Sect. 4.2). Equivalent definitions are found in the bibliography and can be easily converted to $A_{flux\ ratio}$, as e.g.: $A = \frac{S_l - S_h}{S_l + S_h}$ (Matthews et al. 1998) and $E1 = 10 \times (1 - 1/A_{flux\ ratio})$ (Bournaud et al. 2005). We indicate the $A_{flux\ ratio}$ values in Figure 2, 3, and 4 for the examples of H I profiles visually classified as symmetric, CIG 226, slightly asymmetric, CIG 421, and strongly asymmetric, CIG361, which are characterized by $A_{flux\ ratio}$ = 1.05, 1.15, and 1.51, respectively.

3.2.1. Uncertainties of the $A_{flux\ ratio}$

We estimate the uncertainty of the asymmetry index, $\Delta A_{flux\ ratio}$, by taking into account *a*) the *rms noise* per channel, *b*) the uncertainty in the calculation of the *mean velocity*, and *c*) the observational *pointing offsets*:

- *a)* Uncertainty owing to the rms of the H I profile (ΔA*(rms)*): owing to the rms of the spectrum, σ, the uncertainty in S_l is $\Delta S_l = \sqrt{N_l}\sigma R$, where N_l is the number of channels corresponding to S_l and R is the spectral resolution of the profile. The uncertainty in S_h, ΔS_h can be obtained in the same way. Then $\Delta A_{flux\ ratio}$ can be calculated as $\Delta A_{flux\ ratio} = [(\frac{1}{S_h}\Delta S_l)^2 + (\frac{S_l}{S_h^2}\Delta S_h)^2)]^{1/2}$.
- *b)* Uncertainty owing to the measurement of the mean velocity (ΔA*(mean vel)*): since the $A_{flux\ ratio}$ is calculated as an areal ratio obtained from the mean velocity, an error in the determination of the latter can induce a wrong measure of $A_{flux\ ratio}$. An error ΔV_m in the estimate of the mean velocity V_m produced by limited velocity resolution and/or S/N ratio would artificially increase the asymmetry index of a symmetric profile (i.e. $A_{flux\ ratio} = 1$). Namely $A_{flux\ ratio} = \frac{S_l + \epsilon}{S_h - \epsilon} > 1$. A good estimate of the uncertainty can be obtained from the increase in $A_{flux\ ratio}$ for a symmetric profile. If the profile were symmetric, then S$_l$ = S$_h$ = $S/2$, where A is the total area under the profile. ϵ can be estimated as $\epsilon \sim h\ \Delta V_m$, where h is an intensity height scale. The uncertainty of ΔV_m can be estimated as $\Delta V_m = 4\frac{\sqrt{R\ P}}{S/N}$ (Fouque et al. 1990), where $P = (W_{20} - W_{50})/2$, parameter that represents the steepness of the edges of the H I profile, and W_{20} and W_{50} are the widths at 20% and 50% with respect to the peak, respectively. Owing to the uncertainty in the determination of V_m, we can express ΔS_l (and ΔS_h) as: $\Delta A_l = \Delta A_h = 4\frac{\sqrt{R\ P}}{S/N}h$, where we estimated that $h = h_{max}/2$, being h_{max} the H I profile strongest peak.
- *c)* Uncertainty owing to pointing offsets (ΔA*(pointing offset)*): a pointing offset of the antenna with respect to the kinematic center of the galaxy can induce an artificial lopsidedness in the H I profile when the telescope beam is comparable to the size of the galaxy (e.g. Tifft & Huchtmeier 1990; Springob et al. 2005). In some cases the observing coordinates were not coincident with the center of the galaxies owing to errors in the positions found in the CIG (e.g. Leon & Verdes-Montenegro 2003). The expected flux loss (f) owing to beam attenuation *and known antenna pointing offsets* can be calculated from the optical diameter of the galaxy, beam size, and pointing (Springob et al. 2005). We decomposed the expected flux loss (f) into two components, $f = f_{b.a.}\ f_{p.o.}$, where $f_{b.a.}$ is the flux loss factor arising from beam attenuation and $f_{p.o.}$ is the factor where the contribution of the pointing offset is. The latter is intimately related to the flux loss that contributes to the asymmetry of the H I profile. Note that beam attenuation with no pointing offset causes no asymmetry in the H I profile. The difference in the $A_{flux\ ratio}$ parameter if the flux loss that contributes to the asymmetry is on the receding or approaching side provides a measure of ΔA*(pointing offset)*. We find among the H I profiles only eight galaxies (out of the 312) that have differences larger than 0.01. The average is a factor 10 smaller than the contribution from the other two sources of uncertainty. The average is 0.001 and the standard deviation is 0.004. Thus, this source of error is negligible in most cases in our data. This is a result of the small known pointing offsets in the observations, where the average is equal to 3″ and the standard deviation is 3″.

We added these sources of uncertainty in quadrature to estimate the net uncertainty in $A_{flux\ ratio}$, $\Delta A_{flux\ ratio}$.

3.2.2. Other possible sources of uncertainty

In addition to these sources of uncertainty, there are other effects that can induce an artificial asymmetry on the H I profiles. These include the effect of *random* pointing offsets and baseline fitting.

Flux loss due to this effect must be somewhere between $\lesssim$ 1% (GBT, Haynes et al. 1998) and 5% (Arecibo circular feed, Haynes & Giovanelli 1984). If the profile were initially symmetric, then the induced asymmetry parameter by this effect would be in the range $A_{flux\ ratio} < 1.02 – 1.11$, if all flux loss is located either in the receding or approaching sides. Because we have data from different telescopes, our situation is probably intermediate between both cases. We assume that the resulting $A_{flux\ ratio}$ distribution of a sample with symmetric H I profiles observed under similar conditions as our sample is likely well represented by a half-Gaussian with a $\sigma = 0.04$.

The baseline fitting process can also produce artificial asymmetries in the H I profiles (Haynes et al. 1998). Haynes et al. (1998) indicate that different order fits show flux differences of about 3%. As a result, the asymmetry parameter for symmetric H I profiles can be altered up to $A_{flux\ ratio} = 1.06$. A half-Gaussian curve with $\sigma = 0.02$ would mimic this effect well.

Given the random nature of these two effects, we cannot estimate their values individually, but their overall effect is taken into account in Sect. 6 to discuss the actual shape of the $A_{flux\ ratio}$ distribution in isolated galaxies because they can broaden the resulting distribution.

3.2.3. Presentation of the asymmetry data

We list in Table 1 the following information:

- *1)* CIG number;
- *2)* Visual classification: 0 = symmetric, 1 = slightly asymmetric, and 2 = strongly asymmetric (Sect. 3.1),
- *3)* $A_{flux\ ratio}$, the asymmetry parameter (Sect. 3.2),
- *4)* $\Delta A(rms)$, the uncertainty in $A_{flux\ ratio}$ owing to the rms of the H I profile (Sect. 3.2.1),
- *5)* $\Delta A(mean\ vel)$, the uncertainty in $A_{flux\ ratio}$ owing to the mean velocity (Sect. 3.2.1), and
- *6)* $\Delta A_{flux\ ratio}$, the global uncertainty in $A_{flux\ ratio}$, including the small contribution from $\Delta A(pointing\ offset)$ (Sect. 3.2.1).

The $A_{flux\ ratio}$ distribution is shown in Figure 5. The best half-Gaussian fit[2] to the asymmetry parameter distribution is characterized by a $\sigma = 0.15$. However, this half-Gaussian fit is not able to reproduce the $A_{flux\ ratio}$ distribution both at the high and low ends. First there is an excess of high values of $A_{flux\ ratio}$ with respect to the Gaussian curve, and second, the peak of the distribution is too flat for $A_{flux\ ratio} < 1.15$.

We show in Figure 6 *a* and *b* the $\Delta A(rms)$ and $\Delta A(mean\ vel)$ distributions, respectively. The combined effect of all the previous uncertainties, $\Delta A_{flux\ ratio}$ (including the small contribution of $\Delta A(pointing\ offset)$), is shown in Figure 6 *c*. We show the best Gaussian fits to the distributions.

3.3. *Comparison between the visual classification and $A_{flux\ ratio}$*

We compare the asymmetry visual classification of the H I profiles (Sect. 3.1) with the $\mathrm{A}_{flux\ ratio}$ in Figure 7. Three clearly distinct $\mathrm{A}_{flux\ ratio}$ distributions are seen for those galaxies visually classified as symmetric, slightly asymmetric, and strongly asymmetric (Sect. 3.1). The $A_{flux\ ratio}$ distribution of H I profiles visually classified as symmetric has a mean value equal to 1.08, with a standard deviation of 0.065. The distribution for the slightly asymmetric H I profiles is characterized by a larger mean of 1.13 and a similar standard deviation, 0.09. The distribution of strongly asymmetric profiles is characterized by a mean of 1.37 and a considerably larger scatter, 0.17, with values as high as $A_{flux\ ratio} = 1.8$. The $A_{flux\ ratio}$ distribution for the slightly asymmetric subsample partially overlaps with those of the symmetric and asymmetric distributions.

The large overlap that exhibits the $A_{flux\ ratio}$ distribution for each visually classified subsample is not surprising, because this visual classification is of course subjective, and because the $A_{flux\ ratio}$ parameter misses a few cases where the shape of a real asymmetric profile does not correspond to different areas in the approaching and receding sides. Future work would require to inspect other asymmetry parameters that are sensitive to flag these profiles as asymmetric.

3.4. H I *refined subsample and characterization of the $A_{flux\ ratio}$ distribution in a sample of isolated galaxies*

The shape of the $A_{flux\ ratio}$ distribution might be affected by artificially induced values from the effects explained in Sect. 3.2.1. By reducing the net uncertainty in the asymmetry measurement, we reduce errors that might bias our results. We show in Figure 8 how the $A_{flux\ ratio}$ distribution changes for different $\Delta A_{flux\ ratio}$ limits. The smaller the limit (i.e., only including accurate values of $A_{flux\ ratio}$), the better a half-Gaussian reproduces the distribution.

From now on we choose those H I profiles with $\Delta A_{flux\ ratio} < 0.05$, namely the H I refined subsample, to remove from our statistical analysis those profiles with an uncertain determination of the asymmetry index. With this criterion we still have a large sample of $N = 166$ galaxies. The basic property distributions (velocity, morphological type, L_B and L_{FIR}) of the H I refined subsample are shown in Figure 1 as (blue) solid lines, in comparison to those of the H I sample.

In order to characterize the intrinsic scatter of the asymmetry parameter distribution in a sample of isolated galaxies with minor contamination of artificially asymmetric H I profiles we fitted a half-Gaussian function to the H I refined subsample (Fig 9). The fit yields a width of $\sigma = 0.13$ (Fig 9). This time the fit successfully reproduces the asymmetry parameter distribution, including the low and high ends. Only 2% of the isolated galaxies are in excess of 3σ.

The width of the half-Gaussian distribution sets an upper limit to the intrinsic dispersion of the H I asymmetry in isolated galaxies. Errors in the calculation of the asymmetry index might be typically ~ 0.03 (mean of the Gaussian fit) (Sect. 3.2.3). As discussed in Sect. 3.2.2, there might also be random errors in the pointing (~ 0.04) and baseline subtraction ($\sigma \sim 0.02$) that may increase errors in $A_{flux\ ratio}$. Hence it is reasonable to expect a lower value of the width, $\sigma \sim 0.11$, once these sources of errors are corrected.

Note that the quantification of the asymmetry distribution for the galaxies in the H I refined subsample is not affected by inclination effects (e.g. Jog & Combes 2009). Figure 10*a* shows that the inclination of the galaxies are distributed homogeneously above $i = 30^{\mathrm{o}}$. Only two galaxies have an inclination $i < 15^{\mathrm{o}}$ (CIG 85 and 178). The lack of galaxies below $i = 30$ is caused by the width-to-channel ratio criterion explained in Sect. 2.1. This homogeneity in the inclination ensures that most of our galaxies do not show symmetric profiles because the galaxies are viewed face-on, where an asymmetry in the velocity field would remain unnoticed. To further inspect whether inclination can be introducing any bias in our results, we plotted the asymmetry index versus the inclination (Figure 10*b*) and found that the two quantities are not correlated.

---

[2] We fitted the parameters A, μ and σ in a half-Gaussian curve defined as $|A\ \exp(\frac{-(x-\mu)^2}{2.\sigma^2})|$

4. H I profile lopsidedness and environment

4.1. H I *asymmetries and isolation parameters in CIG galaxies*

A reevaluation and quantification of isolation degree for CIG galaxies was reported in Verley et al. (2007c,b). Verley et al. (2007c) derived two isolation parameters for each CIG galaxy: 1) a local surface density parameter η_K within the distance to the k-th neighbor (a good tracer of average galaxy surface density) and 2) a tidal strength parameter Q (a parameter more sensitive to one-on-one interactions).

H I is known to be a sensitive diagnostic of interaction motivating us to compare these two parameters with our $A_{flux\ ratio}$ asymmetry parameter. Figure 11 shows the lack of correlation between $A_{flux\ ratio}$ and both η_K and Q. The Pearson's correlation coefficient is ρ = -0.005 and 0.114, respectively, which indicates that the two quantities are essentially not correlated. A small trend in the Q parameter might be present in the sense that larger H I asymmetries seem to be found in less isolated systems. The calculated intercept and slope are -3.3 ±0.7 and 0.8 ± 0.7, respectively.

The lack of correlation suggest that we are minimizing nurture effects that might affect the H I shape. The low values and small range in terms of galaxy density and tidal strength covered by CIG galaxies are not enough to see a correlation.

Bournaud et al. (2005) also suggest that there is no correlation between lopsidedness and tidal strength. However, they use the lopsidedness A_1 parameter on NIR surface density, and NIR emission is not as extended as the H I.

4.2. H I *asymmetry distribution in field samples*

We compare the asymmetry distribution of our H I refined subsample with that of different studies from the bibliography where a similar asymmetry index (Sect. 3.2) has been calculated and involve field/isolated galaxies (see also Sect. 1) : Haynes et al. (1998), Matthews et al. (1998) and Bournaud et al. (2005).

Figure 12 shows the $A_{flux\ ratio}$ normalized distribution for our refined subsample with 1) Bournaud et al. (2005) and 2) a combined sample (N = 186) including H I data in Matthews et al. (1998), Bournaud et al. (2005), and Haynes et al. (1998) excluding CIG galaxies (80 galaxies). The H I refined subsample shows the distribution best described by a half-Gaussian. It also shows the lowest absolute value of σ. The Bournaud et al. (2005) distribution shows the widest distribution (σ = 0.23) and noticeably deviates from a half-Gaussian curve. An intermediate case, σ = 0.17, is found for the combined sample without CIG galaxies. Table 3 gives σ values for each distribution as well as an asymmetry rate with "asymmetric" profiles defined as $A_{flux\ ratio}$ values exceeding the 2σ level of our H I refined subsample ($A_{flux\ ratio}$ = 1.26).

Figure 13 compares the $A_{flux\ ratio}$ cumulative probability distribution for our H I refined sample and those of Haynes et al. (1998), Matthews et al. (1998), and Bournaud et al. (2005). In each plot the difference of the two curves indicates the asymmetry rate difference for a given $A_{flux\ ratio}$ limit. Our sample lies below the field samples in almost every bin with differences typically between 10 – 20%. A result more similar to our sample is found for Haynes et al. (1998) likely in part because of the significant fraction of CIG galaxies (23%) included in their sample. Removing the CIG overlap increases both their σ and asymmetry rate.

We performed a χ^2 test to check whether the null hypothesis that any of the three $A_{flux\ ratio}$ distributions is similar to our H I refined sample, could be rejected. Except for Haynes et al. (1998) (χ^2 = 9 and the associated p-value = 0.33) this hypothesis can be rejected. In the cases of Bournaud et al. (2005) and Matthews et al. (1998), χ^2 = 47 (p-value = 2×10^{-7}) and χ^2 = 14 (p-value = 0.09) respectively. The sample differences we find are significant and cannot be ascribed to the refinement of the H I sample (Sect. 3.4). In principle we do not know how much Matthews et al. (1998) and Bournaud et al. (2005)'s observations are affected by systematic errors, but differences involving the same criterion as used in our study would yield an asymmetry rate difference < 5%. Haynes et al. (1998) included only high S/N profiles, avoided pointing problems and quantified baseline problems, suggesting it is reasonable to compare it directly with our H I refined sample. Overall, because of their degree of isolation, our H I refined subsample and Haynes et al.'s show a lower frequency (~ 10 – 20%) of galaxies with asymmetric profiles than in other samples such as Matthews et al. (1998) and Bournaud et al. (2005).

5. Relation between H I profile lopsidedness and optical/FIR properties

In this section we explore possible correlations between the asymmetry index $A_{flux\ ratio}$ and optical properties of the H I refined subsample such as morphology, optical signs of perturbation, optical luminosity (L_B), and far-infrared luminosity (L_{FIR}).

5.1. *Morphology and luminosity*

Figure 14 shows the distribution of $A_{flux\ ratio}$ values for each Hubble morphological class (median, mean, and standard deviation values are indicated). The bins representing the majority of our sample ($T(RC3)$ = 3 to 6, i.e. Sb to Scd) show a fairly large scatter (standard deviation $\sigma\sim$ 0.1). We see a slight decreasing trend in $A_{flux\ ratio}$ toward later-type galaxies.

Studies of the relation between H I lopsidedness and morphological type are rare. Matthews et al. (1998) studied a sample of 30 moderate to low surface brightness (T=6–9) galaxies and found a higher asymmetry rate than for more luminous (and higher surface brightness) late-type spirals. They found (for this type range) that later types were more likely to show larger asymmetries. In the Eridanus group the A_1 parameter as calculated from H I maps is larger for earlier type galaxies, suggesting that tidal interactions generate a higher lopsidedness rate in galaxies undergoing secular evolution toward earlier type (Angiras et al. 2006). This result (i.e., larger asymmetries for earlier types) agrees with the general trend seen in our sample.

We compared the $A_{flux\ ratio}$ with luminosity. More luminous galaxies are slightly more asymmetric (Figure 15, left panel). Figure 15 (right panel) presents the cumulative distribution of $A_{flux\ ratio}$ for the high- and low-luminosity subsamples (Verdes-Montenegro et al. 2005). The two distributions are different at a level of α = 0.05 using a chi square test: χ^2=14 and $p - value$=0.01.

5.2. *Optical signs of interactions*

Here we inspect a possible connection between optical signs of interaction and asymmetries in the H I profiles. Sulentic et al. (2006) revised the optical morphology classification for the CIG sample using POSS2/SDSS data. Although the CIG, the starting sample of AMIGA, has been selected to minimize close neighbors to the target galaxy and thus interactions, still Sulentic et al.'s revision revealed N = 193 objects with nearby companions or signs of distortion likely caused by an interaction. Sulentic et al. (2006) flagged these galaxies as *interacting* in the case of a morphologically distorted system and/or almost certain interacting system or flagged as *possibly interacting* if there was any evidence of interaction/asymmetry with/without certain detection of a close companion.

There is no statistically significant difference in terms of H I profile asymmetry rate between galaxies that are optically classified as interacting and those without any sign of interaction. This result is consistent with the conclusion by Kornreich et al. (2000) and Wilcots & Prescott (2004) that optical asymmetries are not necessarily correlated with a lopsided H I component.

5.3. Bar and spiral strengths

We compared the H I asymmetry parameter with the relative spiral and bar strengths calculated as the maximal torque, or ratio of the maximum tangential force and the azimuthally averaged radial force. This has been obtained for a subsample of N = 96 CIG galaxies by Durbala et al. (2009) using Fourier analysis over spiral and bar components separately (Buta et al. 2003). Figure 16 shows the $A_{flux\ ratio}$ parameter with respect to the relative spiral strength (Q_s). The overlapping sample between our H I refined subsample and the one used by Durbala et al. (2009) is composed of 40 galaxies. Q_s seems to anti-correlate with $A_{flux\ ratio}$: disks with weaker spiral arms show stronger asymmetries (Figure 16). There are six galaxies (CIGs 11, 33, 689, 712, 912, and 931) that are outliers to this relation in the high end of the $A_{flux\ ratio}$ parameter. These are likely galaxies whose H I asymmetry parameter is affected by instrumental effects. On the other hand we do not find any correlation of $A_{flux\ ratio}$ and Q_b. The total strength Q_g is not correlated with $A_{flux\ ratio}$ either, not surprisingly because Q_b and Q_g presents a good correlation (Durbala et al. 2009). The relation between Q_s and $A_{flux\ ratio}$ may originate in the observed trends in Q_s versus $T(RC3)$, because Q_s would be expected to correlate with the latter. However, we did not find a clear trend between Q_s and $T(RC3)$.

The correlation found between $A_{flux\ ratio}$ and Q_s suggests that other samples of galaxies characterized by lower spiral strengths will have higher H I asymmetry rates. This is consistent with the OSU sample (Eskridge et al. 2002), where spiral strength is lower than for the CIG (median equal to 0.132 versus 0.161, respectively) (Buta et al. 2005; Durbala et al. 2009), and have a higher H I asymmetry rate with respect to the H I refined subsample (see Sect. 4.2, and Bournaud et al. 2005).

5.4. FIR luminosities (L_{FIR})

L_{FIR} is a good tracer of the star-formation rate and is related to the environment in the sense that IR luminous galaxies ($L_{FIR} > 10^{11}$ $L_\odot$) are usually interacting or merger systems (Sanders & Mirabel 1996). Unlike other samples of galaxies, our isolated population shows low FIR measures e.g. $\log(L_{FIR})$ peaks from 9.0 – 10.5 with very few (<2%) galaxies above 10.5 (Lisenfeld et al. 2007). The low L_{FIR} values of the CIG sample support our claim that the revised CIG (AMIGA) is a sample with only isolated systems (Lisenfeld et al. 2007). Here we inspect whether the small fraction of IR-luminous systems in our sample corresponds to galaxies with larger H I asymmetries. We find N=165 galaxies in our refined H I sample with IRAS measures, including upper limits. Figure 17 (left panel) presents a slight trend in the sense that more luminous FIR galaxies have more asymmetric H I profiles. Right panel of Figure 17 shows the cumulative probability distribution for $A_{flux\ ratio}$ in three bins: $8.0 < \log(L_{FIR}[L_\odot]) < 9.5$, $9.5 < \log(L_{FIR}[L_\odot]) < 10.0$ and $10.0 < \log(L_{FIR}[L_\odot]) < 11.0$. We also show the distribution for those galaxies (N= 60) with FIR upper limits. The null-hypothesis that the first two bins are similar cannot be rejected (at a level of $\alpha = 0.05$) using a χ^2 square test: χ^2=6 and $p-value$=0.24. On the other hand we find that the $A_{flux\ ratio}$ distributions for the latter two bins are different (χ^2=14, $p-value$=0.008) from each other. We find a 10-20% excess of higher asymmetry values for the most FIR luminous galaxies ($10.0 < \log(L_{FIR}[L_\odot]) < 11.0$). If real, this excess might reflect asymmetries and FIR luminosities simultaneously enhanced by accretion events.

6. Discussion

The CIG sample represents the ∼3% most isolated galaxies in the Catalog of Galaxies and Clusters of Galaxies (CGCG, Zwicky et al. 1961). In these systems the effects of environmental perturbation such as tidal interactions and ram pressure stripping are minimized. The $A_{flux\ ratio}$ distribution of our sample is well described by a half-Gaussian function with a 1σ width of 0.13 (possibly smaller $\sigma \sim 0.11$ if artificially induced effects are reduced). Only 9% of the galaxies show $A_{flux\ ratio} > 1.26$ (2σ) and only 5% $A_{flux\ ratio} > 1.39$ (3σ). If it is reasonable to assume that the distribution of intrinsic asymmetries should show a Gaussian distribution, then that of Figure 9 is as close as we have ever come to isolating that intrinsic distribution. Comparison with field samples clearly shows that effects of nurture result in an excess population of high $A_{flux\ ratio}$ values. This excess population measured as a deviation from the best Gauss fit is negligible in our sample. In isolation it is apparently very unlikely to find galaxies with H I disks showing $A_{flux\ ratio} > 1.39$. The small number of such extreme asymmetric profiles found in our sample show double-peaked profiles with unequal horns. This is in most cases not caused by contamination by gas-rich companions with systemic velocity suitable to create a false or amplified horn. We almost never observe such components in the middle or close to the edges (thus broadening one of the horns in) the H I profile. We are unlikely to find a narrower asymmetry distribution in any galaxy sample.

Unfortunately, using H I profiles does not allow us to distinguish between the roles of geometry and kinematics in producing an asymmetry. Aperture synthesis maps suggest that asymmetry is usually the signature of kinematic lopsidedness although galaxies with lopsided HI distributions are not unknown. The rotation curve on one side of the galaxy is usually steeper than the opposite one. Swaters et al. (1999) estimated from previous H I maps (Broeils & van Woerden 1994; Rhee & van Albada 1996; Verheijen 1997) that the fraction of kinematically lopsided galaxies may be as large as 15–50%. It is likely that the few asymmetric H I disks in our sample present this kinematically lopsidedness. However, to make a quantitative relation, it would be necessary to calibrate (statistically) how asymmetry parameters in 2D maps relate to those 1D parameters using single-dish data.

We searched for correlations between internal properties of galaxies and the measured $A_{flux\ ratio}$ parameter. Although we maximized our sensitivity to internal correlations by removing all galaxies likely to have been affected by external perturbers, we did not find any strong correlations between stellar properties and H I asymmetry. We find a weak correlation between spiral arm strength and H I asymmetry parameter, in the sense that arms are stronger for galaxies with more symmetric H I profiles. The simplest interpretation for such a trend would be that gas asymmetries are more efficiently suppressed by the stronger spiral arm gravitational torques in more massive galaxies. A connection to spiral arm strength rather than to bar features should arise from the larger scale of the former. It has long been known that more developed spiral arms seem to exist in more luminous galaxies (van den Bergh 1960). Interestingly, the morphology of spiral arms is found to depend primarily on parent galaxy properties rather than on the environment (van den Bergh 2002). Therefore we would expect an anti-correlation between H I asymmetry and luminosity. However, Fig. 15 shows a hint of the opposite trend. This might be because unlike van den Bergh's (1960) study, our study focuses on a sample with a small range in luminosity, as shown in Figure 1c.

The lack of a strong correlation between L_{FIR} and $A_{flux\ ratio}$ indicates that the bulk of the star formation and the symmetry of the gaseous disk are not strongly linked, i.e., that induced SF caused by possible interactions in this sample is small compared to that from secular evolution. Still, there is an excess of about 10% of asymmetric profiles for the most IR luminous ($10 < \log(L_{FIR}[\mathrm{L}_\odot]) < 11$) galaxies. This might be linked to recent accretion events in a small number of CIG galaxies.

In general the asymmetry distribution will likely deviate from a half-Gaussian curve for other samples containing galaxies that are perturbed by the environment. These samples are the rule while very isolated galaxies are the exception. The intrinsic asymmetry distribution found in our sample of isolated galaxies will be skewed toward higher values as a result of these interactions. This is confirmed by the wider distributions found in samples of field galaxies (Sect. 4.2) where a higher degree of interaction is expected, given the lack of a strict isolation criterion. The deviation from a half-Gaussian curve for the sample in Bournaud et al. (2005) is apparent as shown in Sect. 4.2, and the distribution is the widest ($\sigma = 0.23$) among those studied. Although it has been known for a long time that interacting galaxies usually show larger H I asymmetries (Sulentic & Arp 1983), a statistical analysis using a common H I profile asymmetry parameter in large and well-characterized samples in dense environments is still needed.

Mapelli et al. (2008) estimate from the density of (collisional) ring galaxies in the local Universe that major asymmetries for ∼ 10% of the galaxies may be produced as a result of a recent fly-by, resulting in a lopsidedness visible over a time scale of 1 Gyr. Within the uncertainties of this estimate, this may well match the 10–20% difference between our sample and field samples. As reviewed in Sect. 1, many mechanisms have been proposed other than tidal interactions or ram pressure from the intergalactic medium that may contribute to the asymmetry parameter distribution, such as minor interactions/mergers (e.g., Zaritsky & Rix 1997), gas accretion along cosmological filaments (Bournaud et al. 2005), halo-disk misalignment (Levine & Sparke 1998; Noordermeer et al. 2001), internal perturbations including sustained long-lived lopsidedness owing to non-circular motions (Baldwin et al. 1980) or global m=1 instabilities (Saha et al. 2007). In principle the latter physical processes are likely to occur homogeneously for any sample independently of its environmental properties. Thus, the intrinsic asymmetry distribution found in our sample of isolated galaxies is likely due to a combination of these processes. Owing to the lack of spatial resolution in our data, at this moment we cannot distinguish their respective importance. High-resolution observations of isolated galaxies are a good probe to shed light into the origin of these more subtle asymmetries, though they are likely widespread in all kinds of environments.

We have started a follow-up study of the origin of H I asymmetries using Very Large Array (VLA), expanded VLA and Giant Meter Radio Telescope (GMRT) aperture synthesis H I observations of a subsample of ∼ 20 isolated galaxies, which will be presented in a forthcoming paper. We selected galaxies covering the wide range of asymmetries found in our sample. One of the isolated galaxies presenting an asymmetric profile in this subsample is CIG 96 (NGC 864), whose H I synthesis imaging from the VLA has been studied in detail in Espada et al. (2005). The asymmetry in the H I profile is associated with a strong kinematical perturbation in the gaseous disk of the galaxy, where on one side the decay of the rotation curve is faster than Keplerian. Although a companion is detected, no tidal tail is found, and it is probably not massive enough to have caused this perturbation. Probably we are witnessing the recent merger of a small gaseous companion.

7. Summary and conclusions

We used H I global velocity profiles for a large sample of isolated galaxies to *i*) quantify the rate and amplitude of H I asymmetries in isolated spiral galaxies, where environmental processes such as tidal interactions and ram pressure are minimized, *ii*) study the role of the environment on the H I asymmetries, and *iii*) study possible correlations between H I lopsidedness and the properties of the stellar component, including their morphological types, signatures of optical perturbation, bar and spiral strengths, as well as optical and FIR luminosities.

To quantify the H I asymmetry, we calculated a flux ratio asymmetry parameter ($A_{flux\ ratio}$). We restricted our study to a sample of $N = 166$ galaxies (the H I refined subsample) for which we minimized undesired artificially induced lopsidedness by avoiding large uncertainties owing to the rms of the profile, determination of the mean velocity, and pointing offsets.

We found that a half-Gaussian curve properly fits the $A_{flux\ ratio}$ distribution of this refined sample, with a $\sigma = 0.13$. We suggest that if we deconvolve other sources of errors such as baseline fitting and random pointing offsets, then the underlying σ is reduced to $\sigma \sim 0.11$. We confirm that by using this sample we effectively minimize nurture effects, because there is a lack of correlation between H I asymmetries and isolation parameters such as tidal force (one-on-one interactions) and number density.

We compared the distribution of H I asymmetries of previously studied field galaxies with that of our isolated galaxy sample. A half-Gaussian fit does not successfully reproduce in general the asymmetry distribution of field samples. Indeed, the intrinsic σ is larger in field samples than in isolated galaxies. This is likely a result of the lack of an isolation criterion in the selection of field galaxies, which are likely contaminated by interacting objects. This suggests that environmental mechanisms (producing short-lived effects ∼ 1 Gyr) are fundamental mechanisms to produce H I asymmetries in galaxies, and are indeed responsible for the ∼ 10–20% difference in the H I asymmetry rate we see in field galaxies with respect to isolated galaxies. The asymmetry distribution of galaxies in denser environments is likely even wider and more skewed.

Within the isolated galaxy sample, we did not find any strong correlation between the H I asymmetry and internal properties such as the morphological type, optical and FIR luminosities or signature of interaction. A signature of perturbed optical emission is not a necessary condition for the H I profile to be asymmetric, and vice versa. We found a trend for larger H I asymmetries to be located in more FIR luminous galaxies that are likely interacting objects. We also found evidence that galaxies with higher spiral arm strength have lower H I asymmetries.

The here presented H I refined subsample can be used to study the origin of intrinsic H I asymmetries in isolated galaxies, and it is also a baseline for samples of galaxies in denser environments with H I data that are properly evaluated for instrumental effects. This can help to shed light into the relative importance of different environmental and internally generated processes in shaping the H I disks of galaxies.

Acknowledgements. We thank the anonymous referee for a careful reading and very detailed report, which helped to improve this paper significantly. DE thanks U. Lisenfeld, E. Battaner, P. Vilchez, R. Garrido, and E. Perez for useful comments. We appreciate the help of the staff members of the different telescopes that have made this work possible (Arecibo, Effelsberg, Nançay and GBT). We thank Francoise Combes for providing the H I asymmetry parameter list in Bournaud et al. (2005). DE has been supported by a Marie Curie International Fellowship (MOIF-CT-2006-40298) within the 6th European Community Framework Programme. DE, JSM, LVM and SV are supported by DGI Grant AYA 2008-06181-C02 and the Junta de Andalucía (Spain) P08-FQM-4205. This research has made use of the NASA/IPAC Extragalactic Database (NED) which is operated by the Jet Propulsion Laboratory, California Institute of Technology, under contract with the National Aeronautics and Space Administration. We acknowledge the usage of the HyperLeda database (http://leda.univ-lyon1.fr).

References

Allen, R. J., Goss, W. M., & van Woerden, H. 1973, A&A, 29, 447
Angiras, R. A., Jog, C. J., Omar, A., & Dwarakanath, K. S. 2006, MNRAS, 369, 1849
Baldwin, J. E., Lynden-Bell, D., & Sancisi, R. 1980, MNRAS, 193, 313
Beale, J. S. & Davies, R. D. 1969, Nature, 221, 531
Block, D. L., Bertin, G., Stockton, A., et al. 1994, A&A, 288, 365
Bournaud, F., Combes, F., Jog, C. J., & Puerari, I. 2005, A&A, 438, 507
Broeils, A. H. & van Woerden, H. 1994, A&AS, 107, 129
Buta, R., Block, D. L., & Knapen, J. H. 2003, AJ, 126, 1148
Buta, R., Vasylyev, S., Salo, H., & Laurikainen, E. 2005, AJ, 130, 506
de Vaucouleurs, G., de Vaucouleurs, A., Corwin, H. G., et al. 1991, Third Reference Catalogue of Bright Galaxies (Volume 1-3, XII, 2069 pp. 7 figs.. Springer-Verlag Berlin Heidelberg New York)
Durbala, A., Buta, R., Sulentic, J. W., & Verdes-Montenegro, L. 2009, in American Astronomical Society Meeting Abstracts, Vol. 213, American Astronomical Society Meeting Abstracts, 443
Eskridge, P. B., Frogel, J. A., Pogge, R. W., et al. 2002, ApJS, 143, 73
Espada, D., Bosma, A., Verdes-Montenegro, L., et al. 2005, A&A, 442, 455
Fouque, P., Durand, N., Bottinelli, L., Gouguenheim, L., & Paturel, G. 1990, A&AS, 86, 473
Haynes, M. P. & Giovanelli, R. 1984, AJ, 89, 758
Haynes, M. P., van Zee, L., Hogg, D. E., Roberts, M. S., & Maddalena, R. J. 1998, AJ, 115, 62
Huchtmeier, W. 1972, A&A, 17, 207
Jog, C. J. & Combes, F. 2009, Phys. Rep., 471, 75
Karachentseva, V. E. 1973, Astrofizicheskie Issledovaniia Izvestiya Spetsial'noj Astrofizicheskoj Observatorii, 8, 3
Kornreich, D. A., Haynes, M. P., Jore, K. P., & Lovelace, R. V. E. 2001, AJ, 121, 1358
Kornreich, D. A., Haynes, M. P., Lovelace, R. V. E., & van Zee, L. 2000, AJ, 120, 139
Leon, S. & Verdes-Montenegro, L. 2003, A&A, 411, 391
Leon, S., Verdes-Montenegro, L., Sabater, J., et al. 2008, A&A, 485, 475
Levine, S. E. & Sparke, L. S. 1998, ApJ, 496, L13+
Lisenfeld, U., Verdes-Montenegro, L., Sulentic, J., et al. 2007, A&A, 462, 507
Mapelli, M., Moore, B., & Bland-Hawthorn, J. 2008, MNRAS, 388, 697
Matthews, L. D., van Driel, W., & Gallagher, III, J. S. 1998, AJ, 116, 1169
Miller, E. D., Bregman, J. N., & Wakker, B. P. 2008, ArXiv e-prints
Noordermeer, E., Sparke, L. S., & Levine, S. E. 2001, MNRAS, 328, 1064
Rhee, M.-H. & van Albada, T. S. 1996, A&AS, 115, 407
Richter, O.-G. & Sancisi, R. 1994, A&A, 290, L9
Rix, H.-W. & Zaritsky, D. 1995, ApJ, 447, 82
Sabater, J., Leon, S., Verdes-Montenegro, L., et al. 2008, A&A, 486, 73
Sabater, J., Leon, S., Verdes-Montenegro, L., et al. 2011, A&A
Saha, K., Combes, F., & Jog, C. J. 2007, MNRAS, 382, 419
Sancisi, R., Fraternali, F., Oosterloo, T., & van der Hulst, T. 2008, A&A Rev., 15, 189
Sanders, D. B. & Mirabel, I. F. 1996, ARA&A, 34, 749
Springob, C. M., Haynes, M. P., Giovanelli, R., & Kent, B. R. 2005, ApJS, 160, 149
Sulentic, J. W. & Arp, H. 1983, AJ, 88, 489
Sulentic, J. W., Verdes-Montenegro, L., Bergond, G., et al. 2006, A&A, 449, 937
Swaters, R. A., Schoenmakers, R. H. M., Sancisi, R., & van Albada, T. S. 1999, MNRAS, 304, 330
Tifft, W. G. & Huchtmeier, W. K. 1990, A&AS, 84, 47
van den Bergh, S. 1960, ApJ, 131, 558
van den Bergh, S. 2002, AJ, 124, 786
Verdes-Montenegro, L., Sulentic, J., Lisenfeld, U., et al. 2005, A&A, 436, 443
Verheijen, M. A. W. 1997, Ph.D. Thesis
Verley, S., Combes, F., Verdes-Montenegro, L., Bergond, G., & Leon, S. 2007a, A&A, 474, 43
Verley, S., Leon, S., Verdes-Montenegro, L., et al. 2007b, A&A, 472, 121
Verley, S., Odewahn, S. C., Verdes-Montenegro, L., et al. 2007c, A&A, 470, 505
Walker, I. R., Mihos, J. C., & Hernquist, L. 1996, ApJ, 460, 121
Wilcots, E. M. & Prescott, M. K. M. 2004, AJ, 127, 1900
Zaritsky, D. & Rix, H.-W. 1997, ApJ, 477, 118
Zwicky, F., Herzog, E., & Wild, P. 1961, Catalogue of galaxies and of clusters of galaxies (Pasadena: California Institute of Technology (CIT), —c1961)

Table 1. Asymmetry quantification for the H I sample

CIG	Visual classification	$A_{flux\ ratio}$	$\Delta A(rms)$	$\Delta A(mean\ vel.)$	$\Delta A_{flux\ ratio}$
2	1	1.009	0.065	0.029	0.071
4	1	1.079	0.026	0.015	0.030
8	0	1.080	0.028	0.018	0.034
9	0	1.108	0.027	0.016	0.032
11	2	1.456	0.058	0.037	0.069
...	...	...	...	...	...

Note. 1) CIG number, 2) visual classification (0 = symmetric, 1= slightly asymmetric, 2 = asymmetric), 3) flux ratio asymmetry parameter $A_{flux\ ratio}$, 4) $\Delta A(rms)$: uncertainty owing to the rms of the H I profile, 5) $\Delta A(mean\ vel.)$: $A_{flux\ ratio}$ uncertainty owing to the determination of the mean velocity, and 6) $\Delta A_{flux\ ratio}$, the final derived uncertainty of $A_{flux\ ratio}$, including the effect of pointing offsets. The full list is available in electronic form at the CDS via anonymous ftp to `cdsarc.u-strasbg.fr (130.79.128.5)`, via `http://cdsweb.u-strasbg.fr/cgi-bin/qcat?J/A+A/vvv/ppp` or from `http://amiga.iaa.es`.

Table 2. Comparison between the visual classification and $A_{flux\ ratio}$

Visual classification	N	Mean	Median	σ
Symmetric	141	1.08	1.07	0.07
Slightly asymmetric	126	1.13	1.13	0.09
Asymmetric	45	1.37	1.32	0.26

Table 3. Comparison of the half-Gaussian σ and H I asymmetry rate between samples of isolated/field galaxies

Sample	N	σ	$A_{flux\ ratio} > 1.26$
H I refined subsample	166	0.13	9 %
Haynes et al. (1998)	104	0.13	9 %
Haynes et al. (1998) no CIGs	80	0.13	10 %
Matthews et al. (1998)	30	-	17 %
Bournaud et al. (2005)	76	0.23	22 %
All, no CIGs	186	0.17	16 %

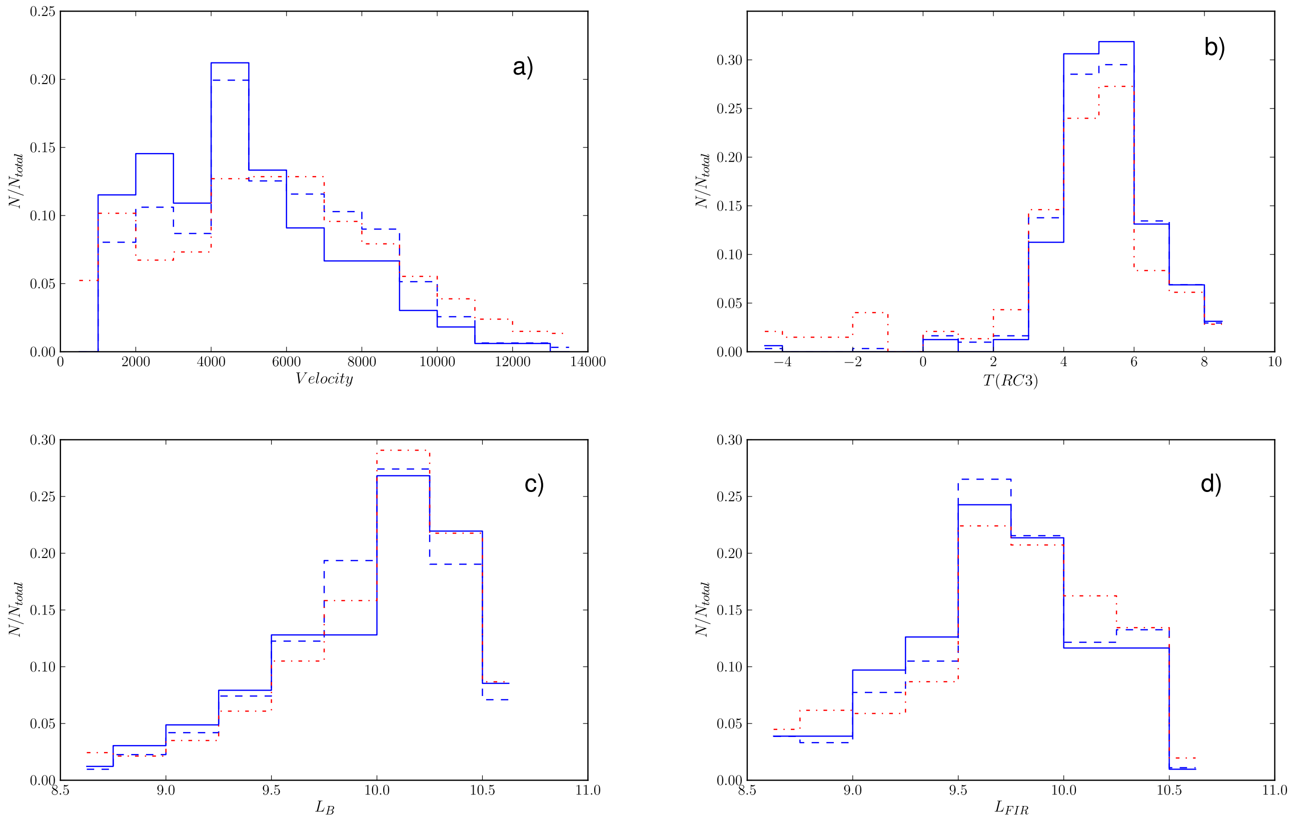

Fig. 1. Basic properties (normalized distributions) of the H I sample (N = 312 galaxies, blue dashed line), the H I refined subsample (N = 166 galaxies, blue solid line), as well as the optically complete sample (Verdes-Montenegro et al. 2005, red dash-dotted line): *a*) velocity (V[km s^{-1}]), *b*) morphology ($T(RC3)$, as in the RC3 catalog), *c*) optical luminosity ($\log(L_B[L_\odot])$) and d) FIR luminosity ($\log(L_{FIR}[L_\odot])$).

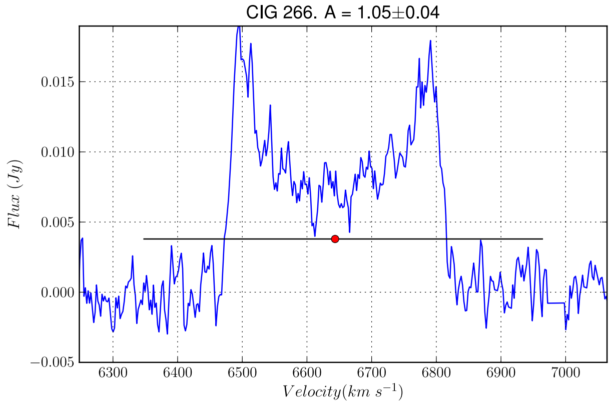

Fig. 2. Example of a symmetric H I profile: CIG 266, $A_{flux\ ratio}$ = 1.05 ± 0.05. The points where the horizontal (black) line intersects the profile correspond to the low (V_l) and high (V_h) velocity ends at a 20% level with respect to the peak. The derived mean velocity (V_m) at a 20% level is plotted as a (red) point.

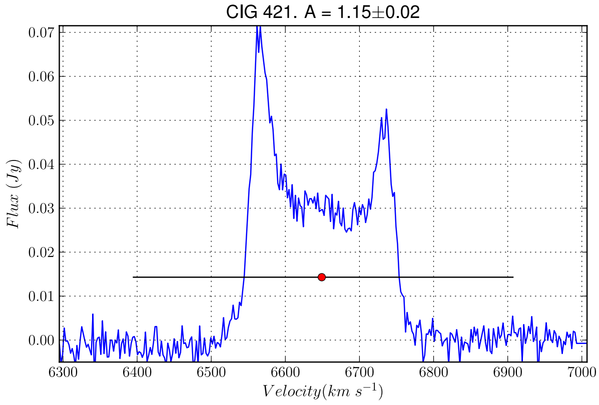

Fig. 3. Example of a slightly asymmetric H I profile: CIG 421, $A_{flux\ ratio}$ = 1.15 ± 0.03. See description in the caption of Figure 2.

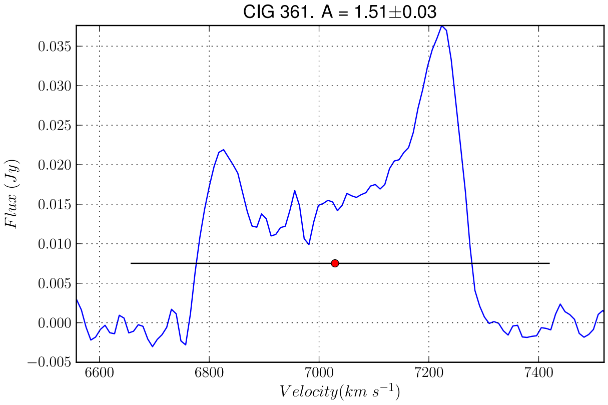

Fig. 4. Example of a strongly asymmetric H I profile: CIG 361, $A_{flux\ ratio}$ = 1.51 ± 0.03. See description in the caption of Figure 2.

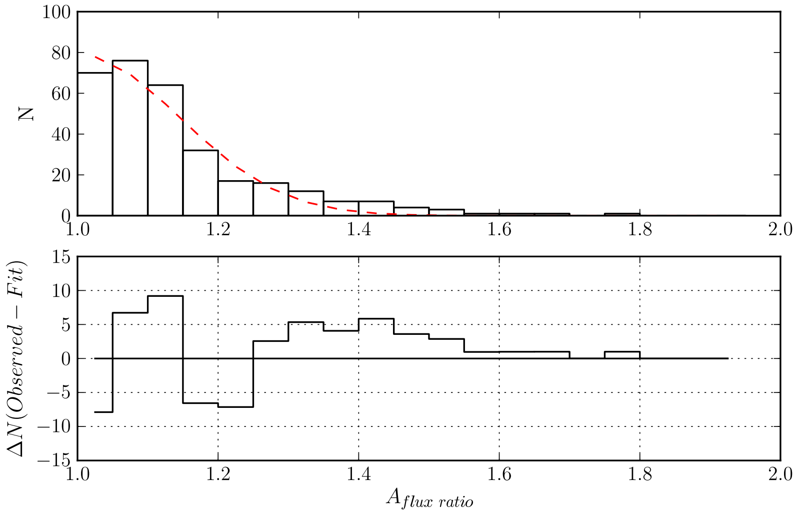

Fig. 5. *Upper panel*) The $A_{flux\ ratio}$ distribution (solid line histogram) of the H I sample (N = 312) and its best half-Gaussian fit (dashed line). *Lower panel*) The residual of the half-Gaussian fit to the observed $A_{flux\ ratio}$ distribution.

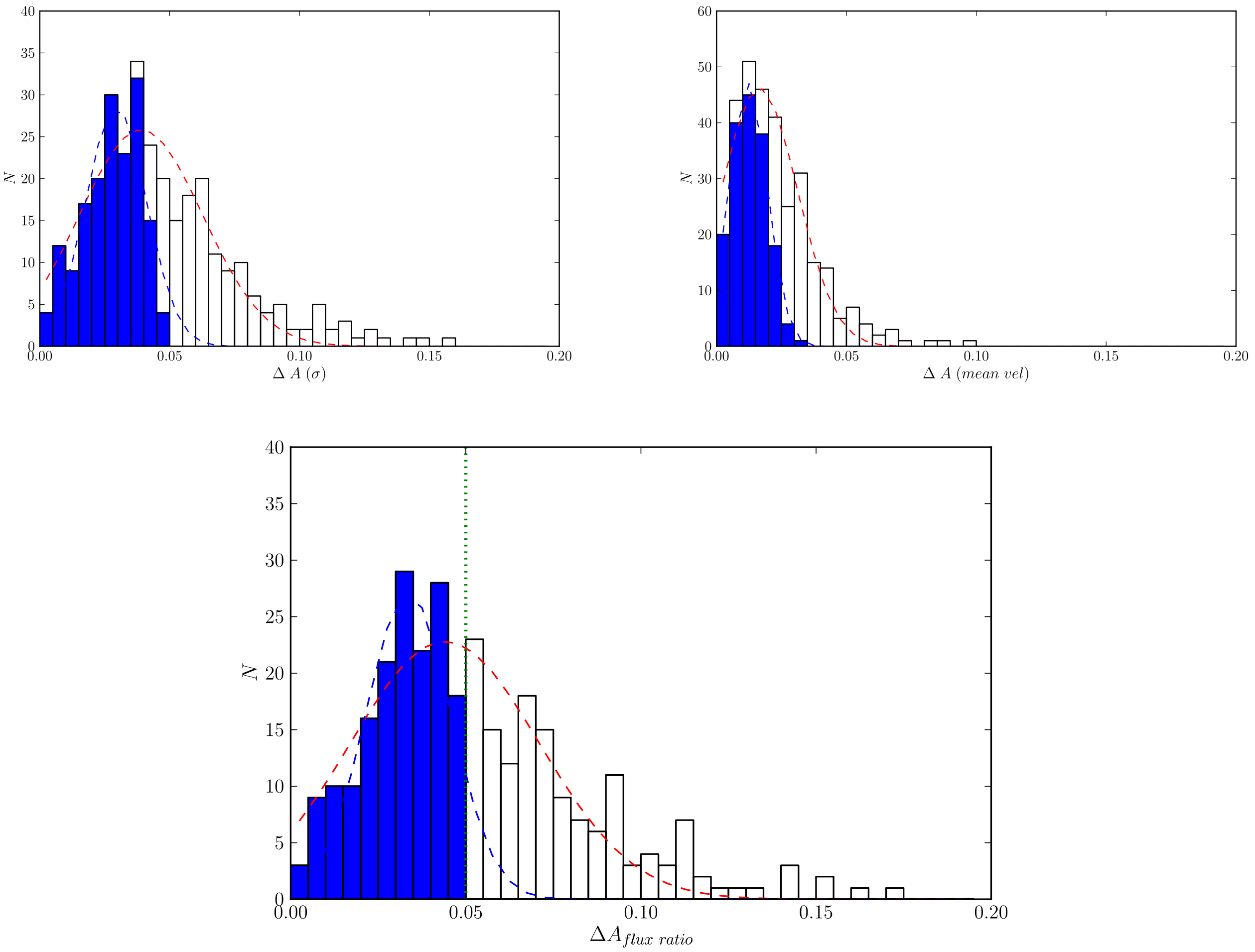

Fig. 6. $Upper\ right$) Uncertainty distribution owing to the rms of the H I profiles, $\Delta A(rms)$. $Upper\ left$) Uncertainty distribution produced by errors in the mean velocity, ΔA(*mean vel*). *Bottom*) Uncertainty distribution of $A_{flux\ ratio}$ for the H I sample (N = 312) combining the effect of $\Delta A(rms)$, ΔA(*mean vel*) and the small contribution of $\Delta A(pointing\ offset)$ (See Sect. 3.2.1). The H I refined subsample ($\Delta A_{flux\ ratio} < 0.05$, indicated as a dotted line in the lower panel) is shown in the plots as blue filled histograms. Best Gaussian fits are presented for all distributions as dashed lines: for the H I sample: *a*) μ=0.02, σ=0.02, *b*) μ=0.04, σ=0.02, and *c*) μ=0.04, σ=0.03; and for the H I refined subsample: *a*) μ=0.012, σ=0.007, *b*) μ=0.029, σ=0.012, and *c*) μ=0.033, σ=0.012.

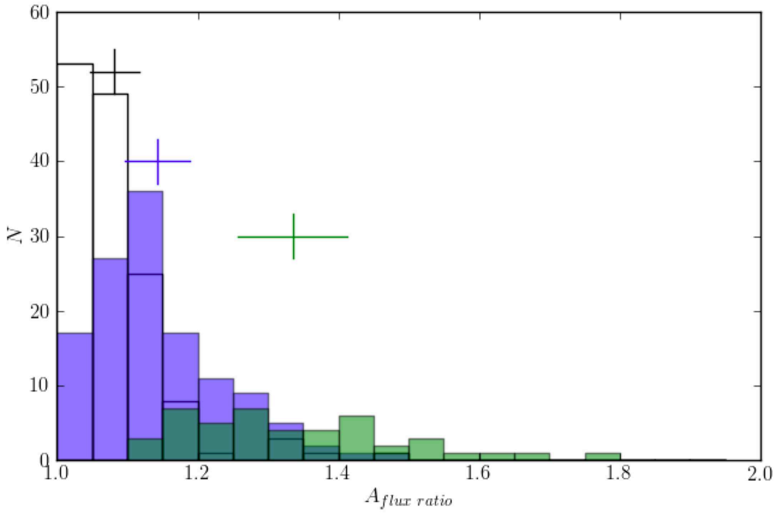

Fig. 7. Comparison between the visual classification and the $A_{flux\ ratio}$ parameter for the N = 312 galaxies in the H I sample (symmetric: white histogram, slightly asymmetric: blue or dark gray histogram, and strongly asymmetric: green or light gray histogram). Mean and standard deviations (σ) for each distribution are also shown by vertical and horizontal lines, respectively.

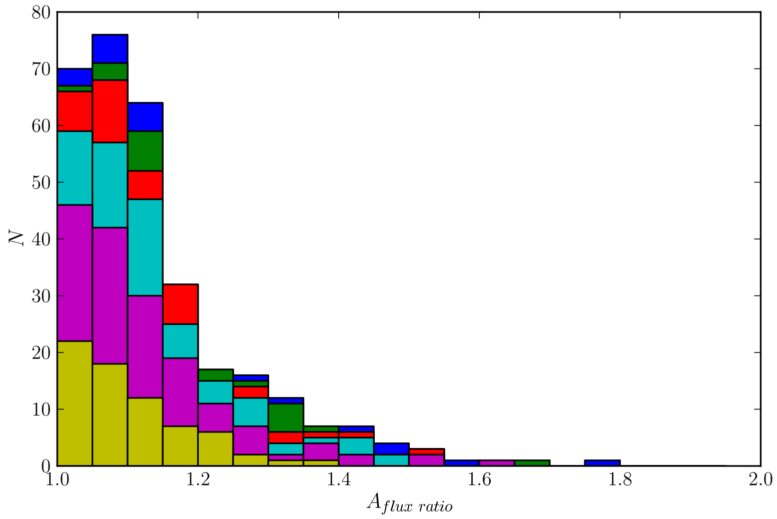

Fig. 8. $A_{flux\ ratio}$ distribution for the different cuts in $\Delta A_{flux\ ratio}$ from 0.03 to 0.11 in bins of 0.02. Note that $\Delta A_{flux\ ratio} < 0.05$ (N = 166, purple filled histogram) corresponds to the H I refined sample (see Sect. 3.4), and the H I sample (N = 312) is the blue solid line histogram.

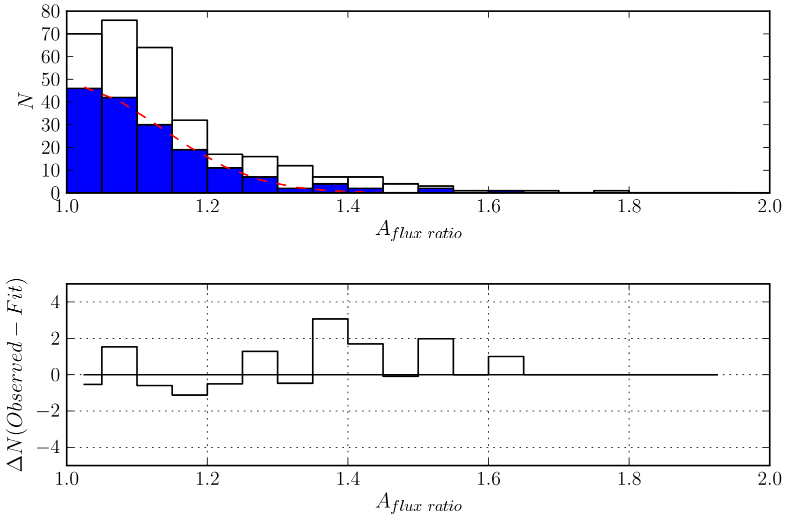

Fig. 9. *Upper panel*) $A_{flux\ ratio}$ distribution of the H I refined subsample ($\Delta A_{flux\ ratio} < 0.05$) ($N = 166$, blue filled histogram), in comparison with that of the H I sample ($N = 312$, solid line histogram) (see Sect. 3.4). A half-Gaussian fit (red dashed line) to the H I refined subsample is presented. The half-Gaussian curve is characterized by a standard deviation σ=0.13, *lower panel*) The residual of the half-Gaussian fit to the observed $A_{flux\ ratio}$ distribution for the H I refined subsample.

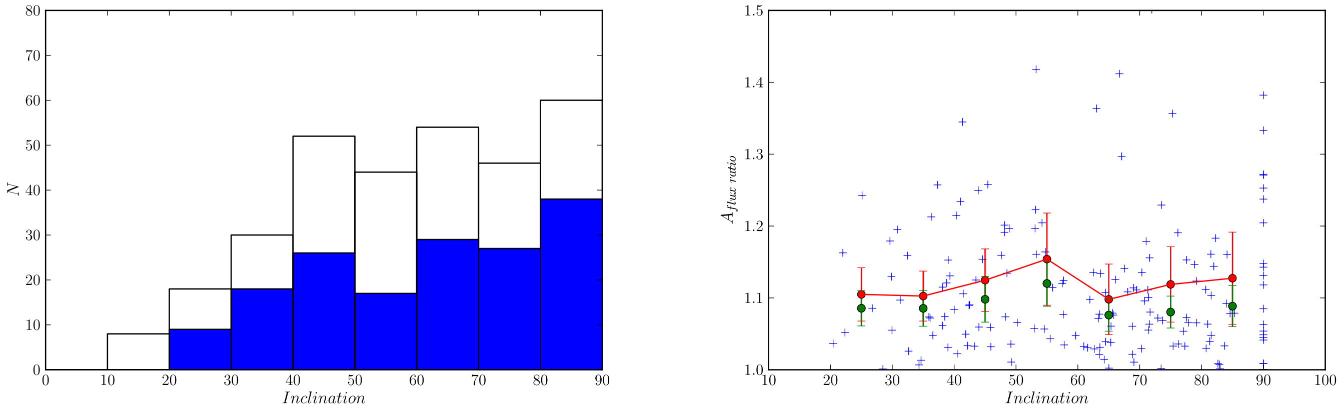

Fig. 10. *a*) Distribution of inclinations for the N = 312 galaxies in the H I sample (solid line histogram) and the H I refined subsample (filled histogram). *b*) $A_{flux\ ratio}$ versus *inclination*, from i = 10 to 90° in 10° bins for the H I refined subsample. Red points and their error-bars indicate the mean (connected by red solid line) and standard deviation, and green points the median and the median absolute deviation.

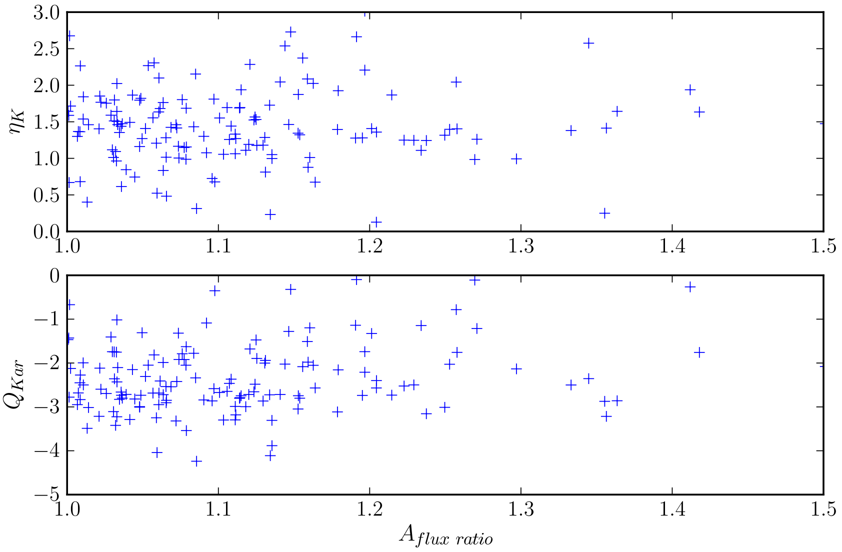

Fig. 11. Isolation parameters vs $A_{flux\ ratio}$. The isolation parameters (Verley et al. 2007b) are the local number surface density parameter η_K to the K-th neighbor, where K = 5 (*upper panel*), and the tidal strength parameter Q (*bottom panel*), which only takes into account similarly size neighbors (factor 4 in size, as defined in Karachentseva 1973).

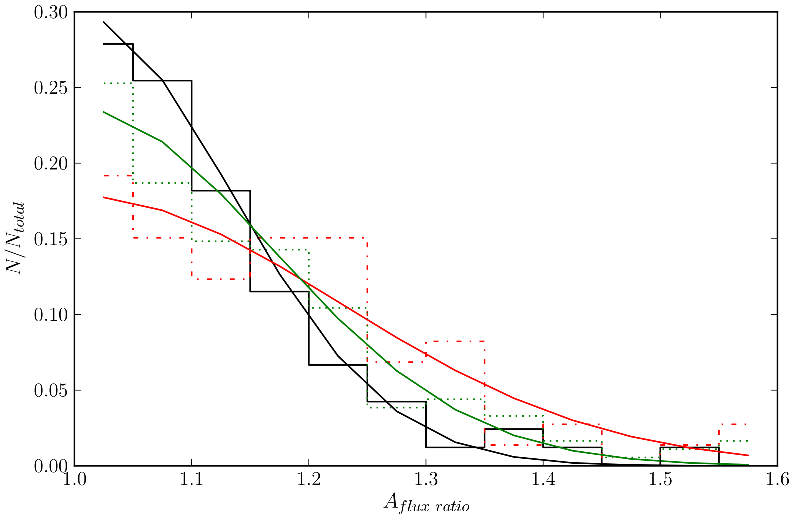

Fig. 12. Comparison of the normalized $A_{flux\ ratio}$ distribution between our H I refined sample (black solid histogram) and 1) Bournaud et al. (2005) (red dotted-dashed histogram), 2) a combined sample including H I data in Bournaud et al. (2005), Matthews et al. (1998) and Haynes et al. (1998) excluding CIG galaxies (green dotted line). Solid curves are the half-Gaussian curves fitted to each distribution. See Table 3 for a comparison of the σ's of each half-Gaussian curve.

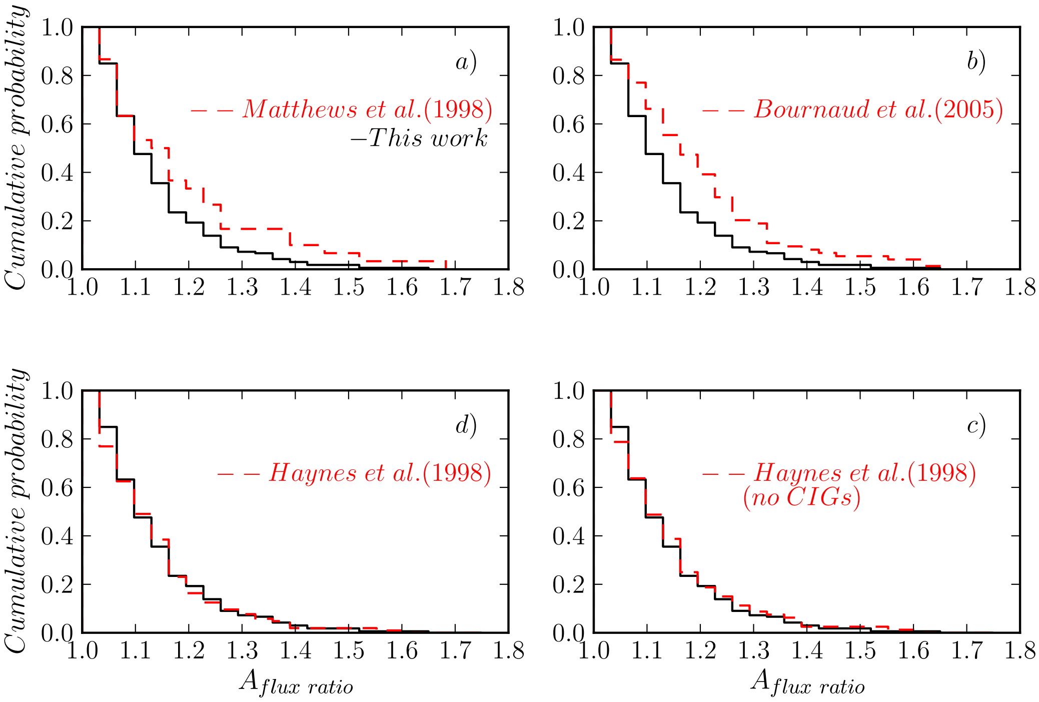

Fig. 13. Comparison of the cumulative $A_{flux\ ratio}$ distribution between our sample (black solid line) and other samples (red dashed lines): *a*) Matthews et al. (1998, $N = 30$), *b*) Bournaud et al. (2005, $N = 76$), *c*) Haynes et al. (1998, $N = 104$)) ($N = 106$), and *d*) Haynes et al. (1998) excluding CIG galaxies ($N = 80$). See Table 3 for an asymmetry rate comparison at a $A_{flux\ ratio} = 1.26$ level.

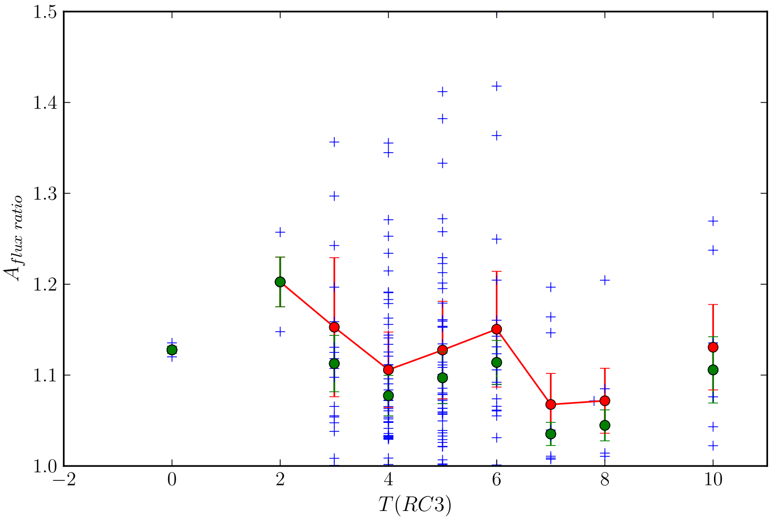

Fig. 14. $A_{flux\ ratio}$ and $T(RC3)$ (Sulentic et al. 2006) for the H I refined subsample. Red points and their error-bars indicate the mean (connected by red solid line) and standard deviation, and green points the median and the median absolute deviation, for each morphological type from $T(RC3)$ = -5 to 10 (E to Im).

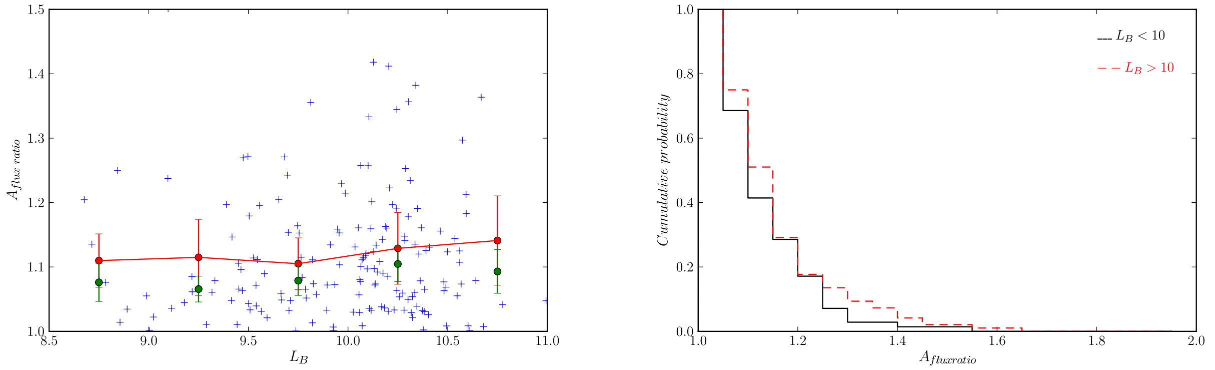

Fig. 15. *Left*) $A_{flux\ ratio}$ versus log($L_B[L_\odot]$). Symbols are as in Figure 14. *Right*) Cumulative probability distribution of $A_{flux\ ratio}$ for log($L_B[L_\odot]$) < 10 (solid line) and log($L_B[L_\odot]$) > 10 (dashed red line), using the H I refined subsample.

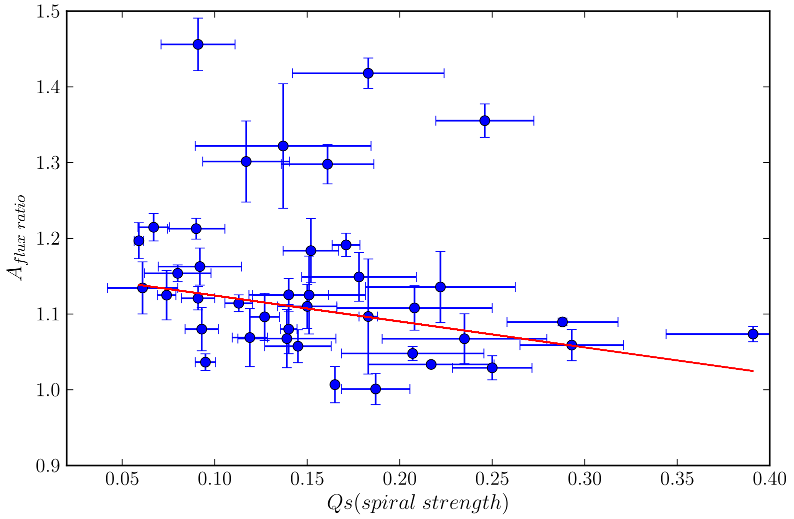

Fig. 16. $A_{flux\ ratio}$ versus spiral strength (Qs) for 40 CIG galaxies overlapping between the H I sample and the CIG galaxies in Durbala et al. (2009). The fit to the data points (slope and intercept are -0.34 and 1.16, Pearson's correlation coefficient ρ = -0.45) is shown as a (red) solid line. The six outliers have been ignored in this fit.

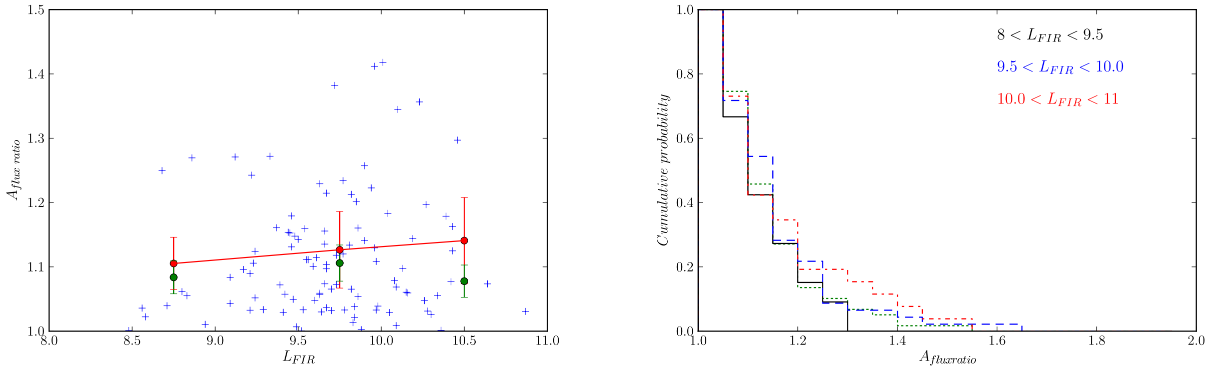

Fig. 17. *Left*) $A_{flux\ ratio}$ versus log($L_{FIR}[L_\odot]$). Symbols are as in Figure 14. *Right*) $A_{flux\ ratio}$ cumulative probability distribution for three L_{FIR} bins: 9 < log($L_{FIR}[L_\odot]$) < 9.5 (solid line), 9.5 < log(L_{FIR} $[L_\odot]$) < 10.0 (blue dashed line) and 10.0 < log($L_{FIR}[L_\odot]$) < 11.0 (dash-dotted line). The (green) dotted line represents the $A_{flux\ ratio}$ cumulative distribution for those galaxies with an upper limit.
.